Indian Association for the Cultivation of Science

Project Report

PHS 5189

Synthesis & Characterizartion of Graphitic Carbon Nitride (g-C_3N_4) Nanosheet

---

by

Katha Haldar

Roll:

2018/UG/012

Under supervision of

Prof. Shyamal Kumar Saha

February 9, 2022

Graphitic Carbon Nitride(g-C_3N_4) Nanosheet

Synthesis & Characterization

Abstract

As a kind of metal free polymer, graphitic carbon nitride is showing a new horizon in the area of nanoscience. Their unique electronic structures, suitable band gap, thermal and chemical stability seem to be a promising candidate for photocatalytic and energy harvesting applications. In this work, graphitic carbon nitride (g-C_3N_4) nanosheet (2D) is produced from melamine and for their structural/microstructural characterization evaluation is done using X-ray diffraction (XRD), scanning & transmission electron microscopy (SEM and TEM), Fourier transform infrared spectroscopy (FTIR) and UV-visible spectroscopy techniques, excitation dependent photoluminescence (PL) spectra.

1. Introduction

Graphitic carbon nitride (g-C_3N_4) is a two-dimensional conjugated polymer that has attracted the interest of researchers and industrial communities owing to its outstanding analytical merits such as low-cost synthesis, high stability, unique electronic properties, catalytic ability, high quantum yield, nontoxicity, metal-free, low bandgap energy, and electron-rich properties. Notably, graphitic carbon nitride (g-C_3N_4) is the most stable allotrope of carbon nitrides.According to the literature, the carbon nitride (CN) material was first studied in 1834 when Berzelius obtained a linear CN polymer and named it "melon". g-C_3N_4can be prepared by the thermal treatment of nitrogen- rich precursors, for example, cyanamide, dicyandiamide, melamine, ammonium thiocyanate, urea and thiourea. However, thermal treatment synthetic methods have some disadvantages.

- The precursors are easily sublimated and this suppressed the g-C_3N_4 to a larger extent at elevated temperatures.
- The strong interactions among different single layers of g-C_3N_4 make it insoluble in most solvents such as water.
- Bulk g-C_3N_4 has low surface area, resulting in limited interaction between g-C_3N_4 and guest species (e.g. biomolecules)

Recently, ultrathin g-C3N4 nanosheets were synthesized by exfoliation of bulkg-C_3N_4 through thermal/chemical oxidation etching and liquid/ultrasonication-assisted exfoliation in polar solvents. For example, Chi et al. obtained highly water-dispersible g-C_3N_4nanoflakes by chemically oxidizing the bulk g-C_3N_4 with nitric acid. Sun et al. prepared ultrathin g-C_3N_4 nanosheets by ultrasonication assisted liquid exfoliation of bulk g-C_3N_4 in water. However, these methods need dangerous reagents or are time-consuming. Thus, developing a facile method is urgently required to produce well dispersed and ultrathin g-C_3N_4 nanosheets.

2. Theory on Different Characterization Techniques :

1. Photoluminescence (PL) spectra
2. UV-visible spectroscopy
3. X-ray diffraction (XRD)
4. Transmission electron microscopy (SEM and TEM)
5. Fourier transform infrared spectroscopy (FTIR)

Photoluminescence (PL) spectra

The analysis of works of art often begins with the visual examination of the surface of an object under UV light. This is because the spectrum of the optical emission from the surface as well as its spatial distribution in a field of view can provide conservators, art historians, and scientists key information regarding the presence of heterogeneities on a painting or a sculpture, signed papers or modern design objects. While the interpretation of fluorescence and the attribution of emissions to specific materials is far from trivial, both the spectrum of the emission, perceived as colour, and the spatial distribution of fluorescence are valuable starting points for further investigations. For example, conservators are experienced at relating differences in the fluorescence of surfaces to damage, to traces of materials (for example organic binders) which may provide insights regarding degradation or to past interventions, to the local applications of varnish (which tends to develop fluorescence with age) or to the presence of retouching (which is often dark when examined under UV light). Many materials found in cultural heritage fluoresce: indeed, stone substrates, organic pigments, binding media and waxes, conservation materials and semiconductors pigments have all been studied using fluorescence spectroscopy.

- Fluorescence is a photoluminescence process in which atoms or molecules are excited by the absorption of electromagnetic radiation. The excited species then relax to the ground state, giving up their excess energy as photons.
- One to three orders of magnitude better than absorption spectroscopy, even single molecules can be detected by fluorescence spectroscopy.
- Larger linear concentration range than absorption spectroscopy.

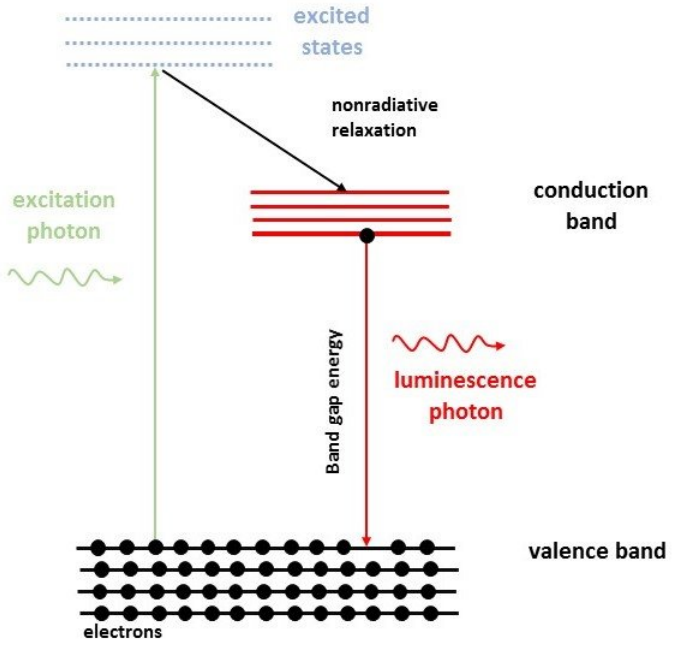

Figure 1: Photoluminescence Process
(Source: www.researchgate.net)

UV-visible spectroscopy

Basically, spectroscopy is related to the interaction of light with matter. As light is absorbed by matter, the result is an increase in the energy content of the atoms or molecules. When ultraviolet radiations are absorbed, this results in the excitation of the electrons from the ground state towards a higher energy state. Molecules containing π-electrons or nonbonding electrons (n-electrons) can absorb energy in the form of ultraviolet light to excite these electrons to higher anti-bonding molecular orbitals. The more easily excited the electrons, the longer the wavelength of light they can absorb. There are four possible types of transitions $\pi - \pi^*, n - \pi^*, \sigma - \sigma^*, n - \sigma^*$) The absorption of ultraviolet light by a chemical compound will produce a distinct spectrum that aids in the identification of the compound.

UV-vis spectroscopic data can give qualitative and quantitative information of a given compound or molecule. Irrespective of whether quantitative or qualitative information is required it is important to use a reference cell to zero the instrument for the solvent the compound is in. For quantitative information on the compound, calibrating the instrument using known concentrations of the compound in question in a solution with the same solvent as the unknown sample would be required. If the information needed is just proof that a compound is in the sample being analyzed, a calibration curve will not be necessary; however, if a degradation study or reaction is being performed, and concentration of the compound in solution is required, thus a calibration curve is needed.

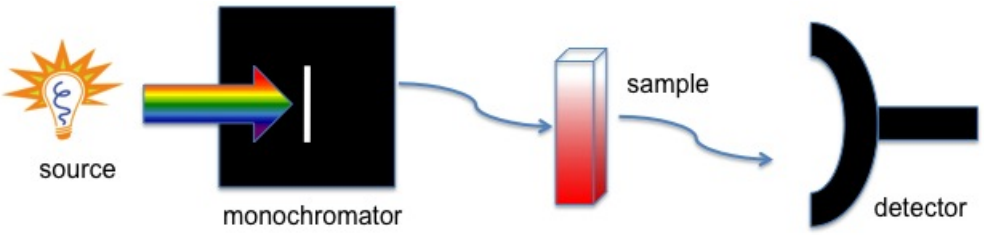

Figure 2: Illustration of a single beam UV-vis
(Source: chem.libretexts.org)

X-ray diffraction (XRD)

English physicists Sir W.H. Bragg and his son Sir W.L. Bragg developed a relationship in 1913 to explain why the cleavage faces of crystals appear to reflect X-ray beams at certain angles of incidence (theta, q). The variable d is the distance between atomic layers in a crystal, and the variable lambda l is the wavelength of the incident X-ray beam; n is an integer. This observation is an example of X-ray wave interference (Roentgenstrahlinterferenzen), commonly known as X-ray diffraction (XRD), and was direct evidence for the periodic atomic structure of crystals postulated for several centuries.

- To measure the average spacings between layers or rows of atoms
- To determine the orientation of a single crystal or grain
- To find the crystal structure of an unknown material
- To measure the size, shape and internal stress of small crystalline regions

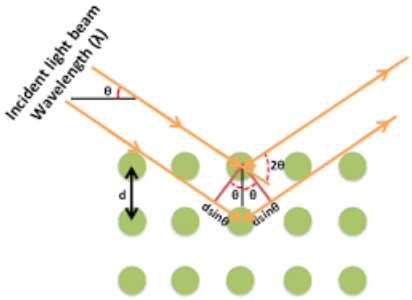

Figure 3: X-ray diffraction (XRD)
(Source: www.researchgate.net)

Transmission electron microscopy (SEM and TEM)

Electron microscopes have emerged as a powerful tool for the characterization of a wide range of materials. Their versatility and extremely high spatial resolution render them a very valuable tool for many applications. The two main types of electron microscopes are the Transmission Electron Microscope (TEM) and the Scanning Electron Microscope (SEM).

The main difference between SEM and TEM is that SEM creates an image by detecting reflected or knocked-off electrons while TEM uses transmitted electrons (electrons which are passing through the sample) to create an image. As a result, TEM offers valuable information on the inner structure of the sample, such as crystal structure, morphology and stress state information, while SEM provides information on the sample's surface and its composition

- TEM images are 2D projections of the sample, which in some cases makes the interpretation of the results more difficult for the operator.
- Due to the requirement for transmitted electrons, TEM samples must be very thin, generally below 150 nm, and in cases that high-resolution imaging is required, even below 30 nm, whereas for SEM imaging there is no such specific requirement.
- Scattering increased with the atomic number and thickness of the sample. For example, contrast in amorphous materials arises from mass-density contrast.

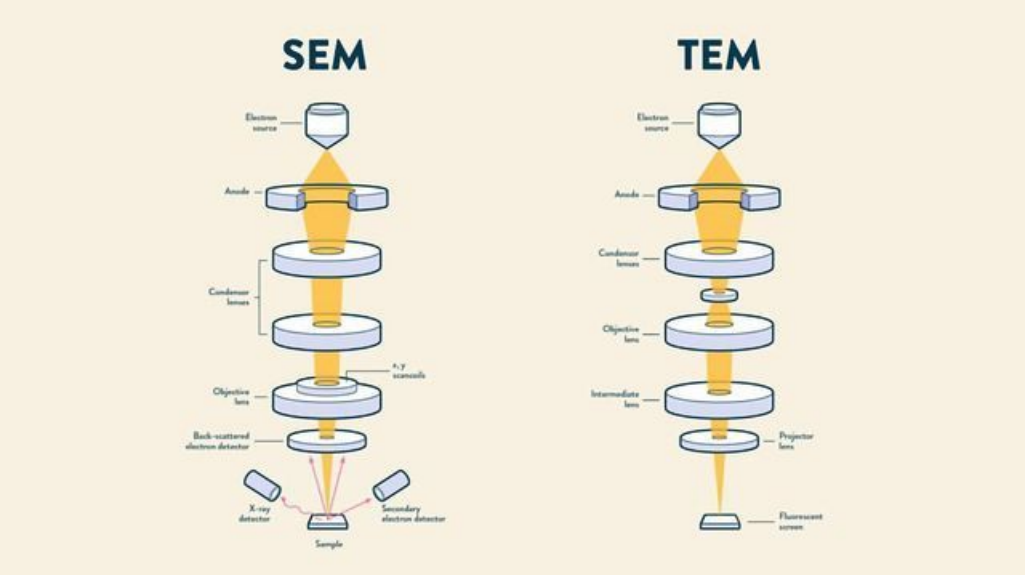

Figure 4: Transmission electron microscopy (SEM and TEM)
(Source: www.researchgate.net)

Fourier transform infrared spectroscopy (FTIR)

Molecular bonds vibrate at various frequencies depending on the elements and the type of bonds. For any given bond, there are several specific frequencies at which it can vibrate. According to quantum mechanics, these frequencies correspond to the ground state (lowest frequency) and several excited states (higher frequencies). One way to cause the frequency of a molecular vibration to increase is to excite the bond by having it absorb light energy. For any given transition between two states the light energy (determined by the wavelength) must exactly equal the difference in the energy between the ground state and the first excited

state. High sensitivity performance with the permanently aligned, high cube corner interferometer, customizable workspaces, hyperspectral imaging,the rmogravimetric coupling, high throughput screening devices and easy measurement mode.

Fourier-transform spectroscopy offers a number of key benefits that have made it the dominant method of IR spectroscopy. When information from all wavelengths is collected at once, there tends to be signal-to-noise ratio reduction in the output spectra. Furthermore, the more obvious benefit of performing all wavelength measurements at once is the speed reduction when compared to dispersive wavelength techniques.

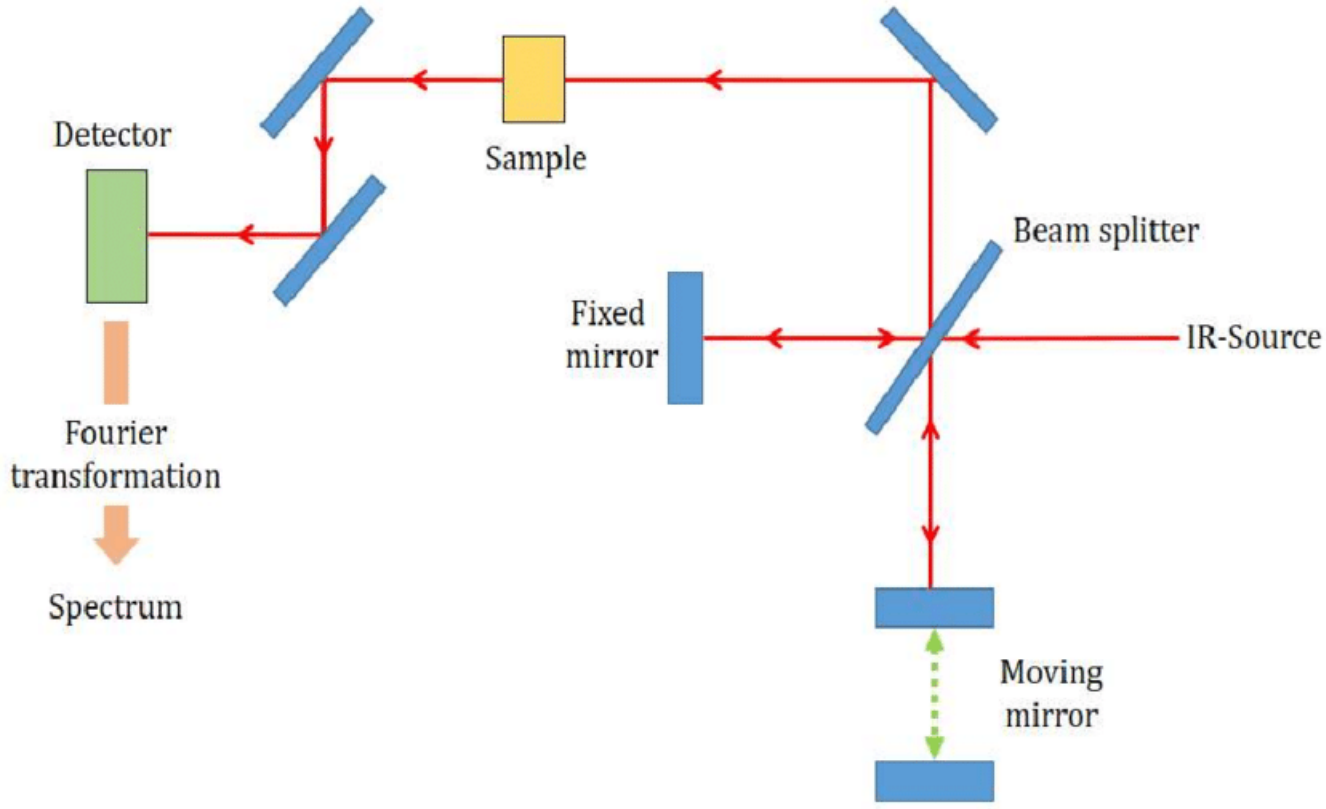

Figure 5: Fourier transform infrared spectroscopy (FTIR)
(Source: www.researchgate.net)

3. Synthesis Procedure of Graphitic Carbon Nitride Nanosheet

The procedure is demonstrated as follows :

- Melamine is heated at 550°C for 6 hours. The process is called Thermal Polycondensation.
- The bulk g-C_3N_4 (yellow) is ground into powder.
- 2 gm of powder is measured.
- It is added into distilled water taken in a test tube.

- The solution is sonicated.
- Excluding the impurities as residue the upper part of the solution is taken
- Then Piranha solution (Sulfuric acid (conc.)and Hydrogen peroxide in 3:1 ratio) is added to the solution.
- The thin film is prepared by drying at moderate temperature.

Figure 6: Thin Film of g-C_3N_4

Figure 7: bulk g-C_3N_4

4. Characterization and Data Analysis

Photoluminescence (PL) spectra

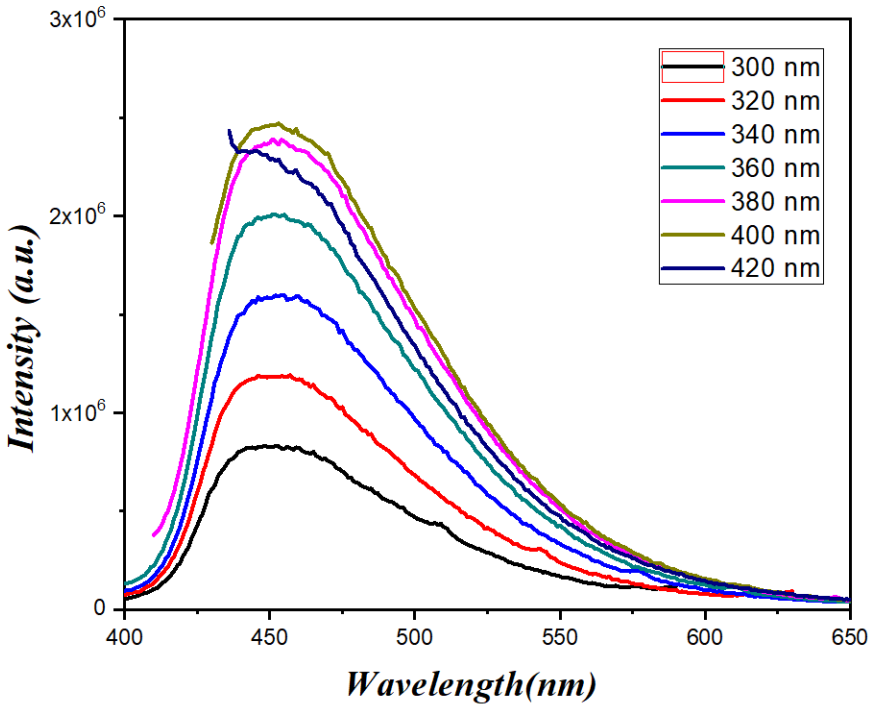

Figure 8: Photoluminescence (PL) emission spectra of g-C_3N_4 Thin Film

Photoluminescence (PL) is a significant and contactless optical method employed to measure purity and crystalline quality, and identify certain impurities in materials for energy

devices. PL spectra of the as-prepared samples are valuable to explain the migration and recombination processes of photo-induced electron-hole pairs. After being activated by the light, photocatalysts can generate electrons and holes, while the photoinduced holes and electrons recombine together, resulting in the energy release in the form of fluorescence emission. Accordingly, it can be inferred that lower fluorescence emission intensity indicates lower recombination rate of electron-hole. It shows a strong intrinsic emission band with a peak at 450 nm, which is attributed to direct electron–hole recombination of band transition. Compared with g-C_3N_4 shows a much weaker emission, implying the recombination of charge carriers may be effectively inhibited by the post-thermal method.

the photon energy of the emitted photon is the direct measurement of energy difference between the involved orbitals or band.

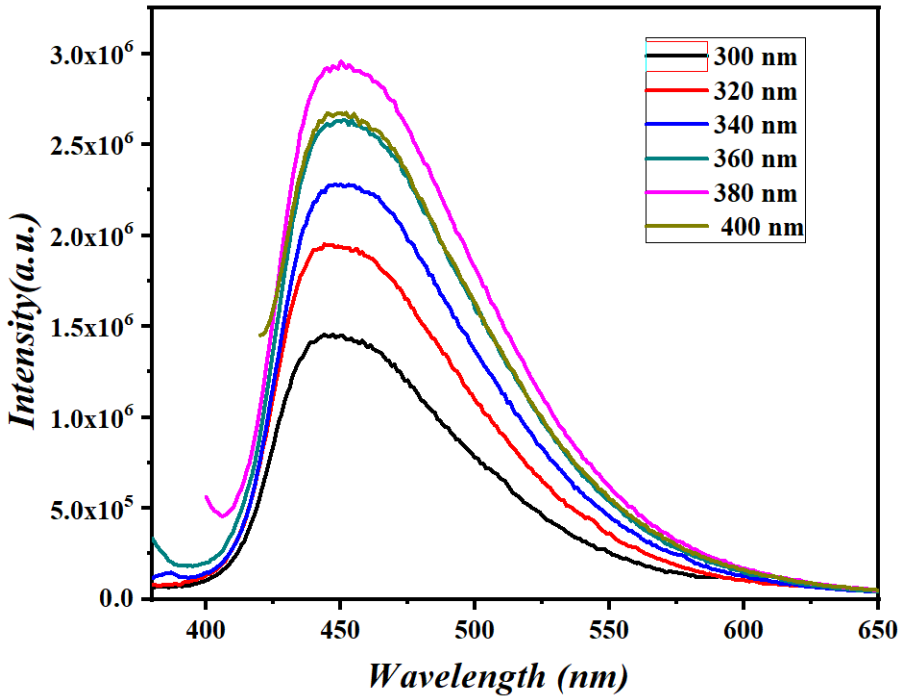

Figure 9: Photoluminescence (PL) emission spectra of g-C_3N_4 in Solution

The fluorescent spectrum shows that the emission band (450-460 nm) remains unchanged for all excitation wavelengths. Nonetheless, the PL emission peak intensity varies with excitation wavelength as shown in Fig. 7b. It was found to increase with increasing the excitation wavelength with maximum intensity at 380 nm. The constant emission wavelength band (450-460 nm) from all the synthesized free-standing g-C_3N_4 films indicate that the g-C_3N_4 films are optically similar. Also, the films show high photostability, with the fluorescence intensity remaining constant after continuous irradiation.

UV-visible spectra of g-C_3N_4

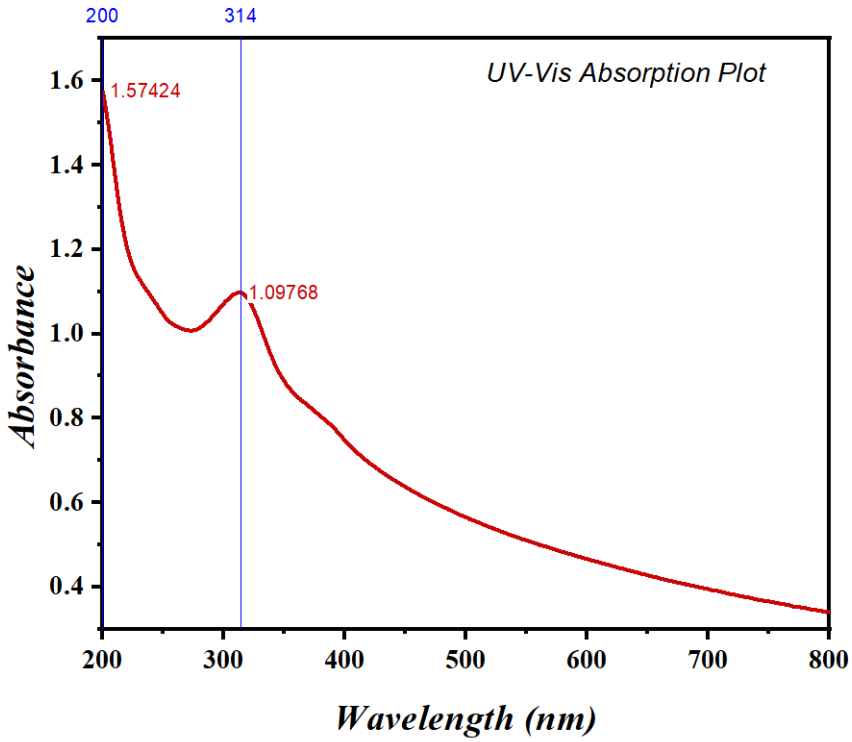

Figure 10: UV-Vis Spectra of g-C_3N_4

lectronic and optical properties are of fundamental importance to determine the photo activity of a catalyst. The absorption properties of synthesized materials were determined by UV-visible (UV-Vis) spectroscopy. The UV-visible spectrum of pure g-C_3N_4 shows an absorption spectrum similar to a typical semiconductor absorption spectrum between 200–450 nm, originating from the charge transfer from a populated valence band of nitrogen atom (2p orbitals) to a conduction band of carbon atom (2p orbitals) of carbon nitride. An additional sharp peak at 200 nm, attributed to the aromatic ring's $\pi - n$ transition, was observed. Another intense peak at 314 nm, due to the $n - \pi^*$ transitions caused by the electron transfer from a nitrogen nonbonding orbital to an aromatic anti-bonding orbital, was also present in the UV-Vis spectrum. The band tailing from 410 to 500 nm suggests a slight visible light absorption capacity of carbon nitride. After doping with phosphorous atoms, the absorption band due to the nitrogen nonbonding to aromatic antibonding $n - \pi^*$ transition was diminished due to the replacement of carbon atoms with phosphorous, whereas the absorption pattern was found to be redshifted due to the better charge contribution by loosely bound electrons of phosphorous in the aromatic conjugated system.

X-ray diffraction (XRD)

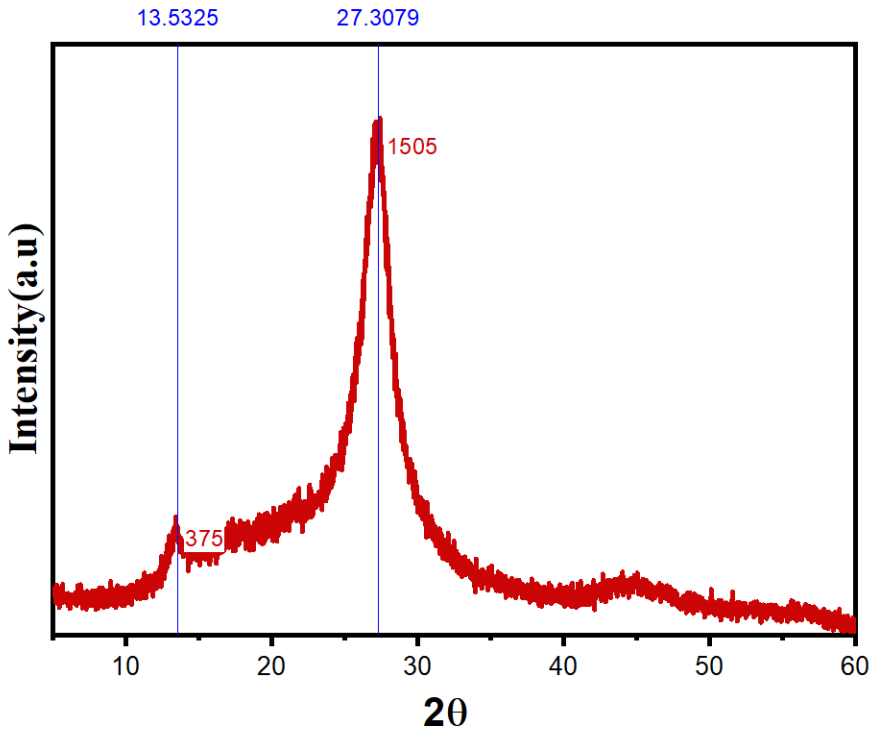

Figure 11: XRD Plot of g-C_3N_4

The observed XRD pattern of the g-C3N4 film, as shown in Fig. 4a, displays two diffraction peaks at 13.53^o and 27.3^o that correspond to the (100) and (002) planes of g-C3N4 respectively. This indicate the graphite-like inter-planar stacking of the conjugated aromatic units of CN that are the characteristic stacking structures of graphitic-like materials (hexagonal g-carbon nitride). We observed the same strong diffraction peaks from all the samples prepared, which indicates that free-standing g-C_3N_4 films with stable crystalline structure were successfully prepared from melamine.

Transmission electron microscopy (TEM)

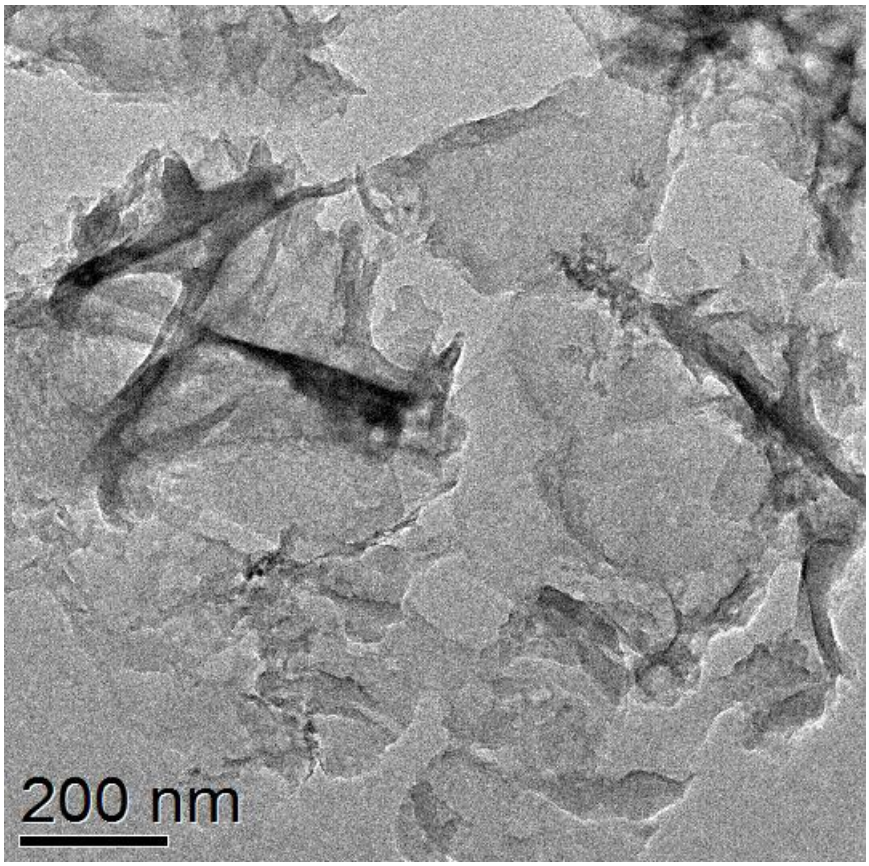

Figure 12: TEM of g-C_3N_4

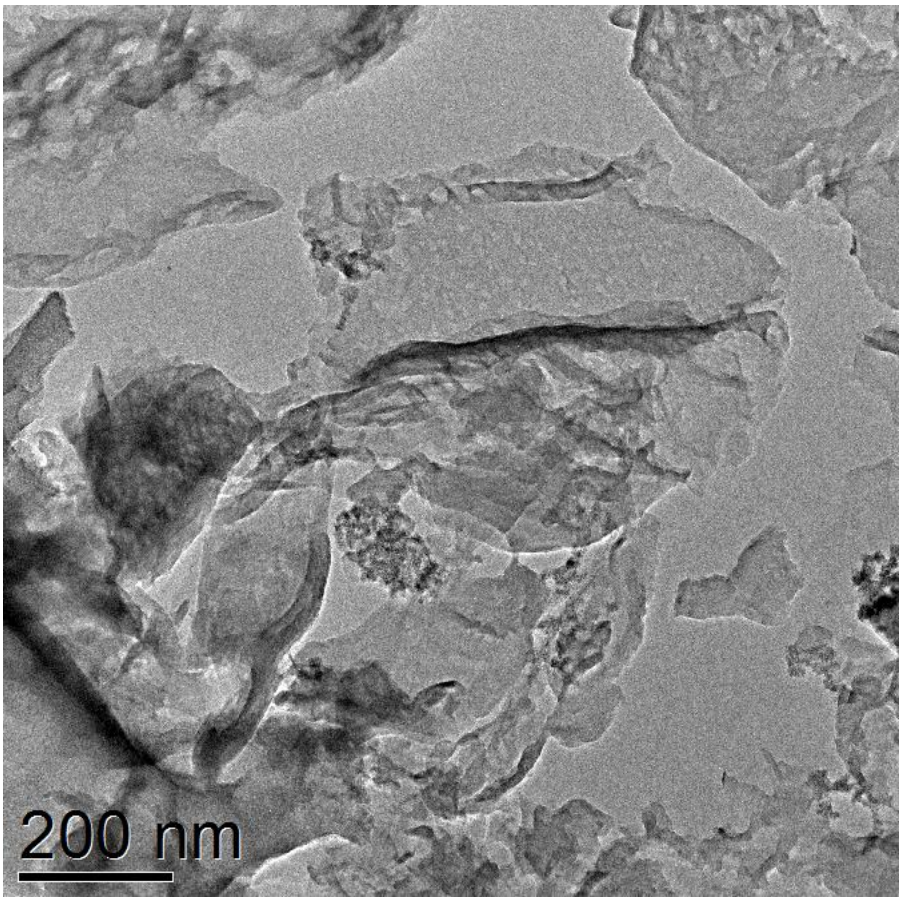

Figure 13: TEM of g-C_3N_4

The synthesized g-C_3N_4 film exhibited the nanosheet structures with top surfaces containing porous morphology with wrinkled flakes. The high magnification images show the nanoporous structures of g-C_3N_4 film and the thickness of the g-C_3N_4 nanolayers is non-uniform.

Fourier transform infrared spectroscopy (FTIR)

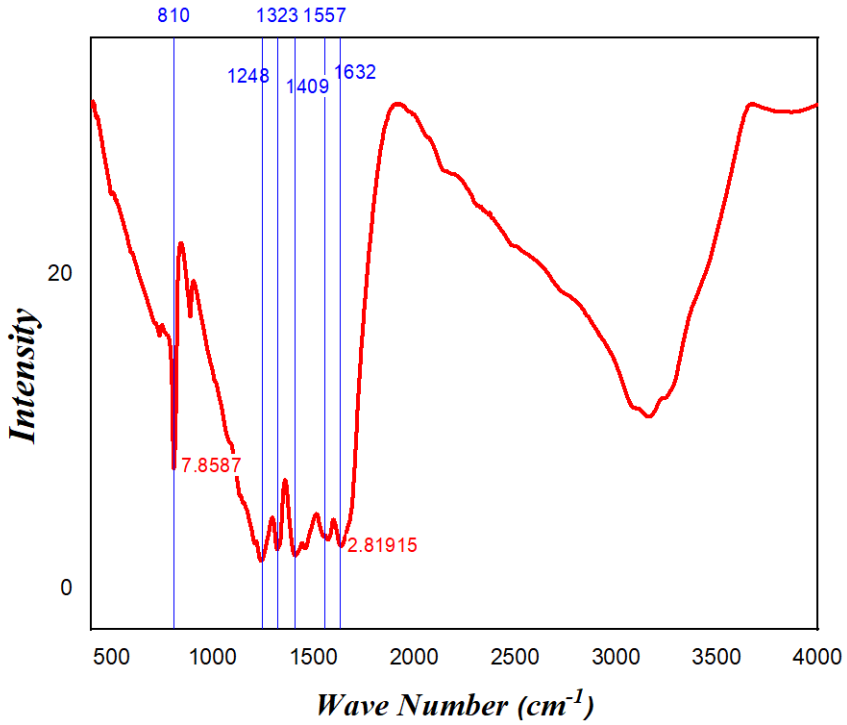

Figure 14: Fourier transform infrared spectra(FTIR) of g-C_3N_4

FT-IR spectroscopy was used to characterize the chemical structure. A typical FT-IR spectrum of the free-standing g-C_3N_4 film is shown in Fig. Several bands are displayed in the region of 4000-700 cm^{-1}, which are characteristic of the C- N stretching. The sharp and intense transmittance band at 817 cm-1 can be attributed to the vibration of triazine rings, indicating the existence of the units with -NH and -NH2 groups. The several peaks in the region from 1200 to 1600 cm^{-1} can be attributed to typical stretching modes of either trigonal C-N (-C)-C or bridging C-NH-C units in g-C_3N_4 film. The broad peaks between 3070 and 3285 cm^{-1} correspond to N-H and O-H stretching and hydrogen-bonding interactions.

5. Conclusion :

In summary, we have developed a facile one-step CVD assisted approach for the synthesis of high-quality and large area. The film was made up of g-C3N4 nanolayers with variable thickness due to folding and overlapping of various nanolayers. The detailed PL spectra and decay analysis obtained with different excitation energies revealed no significant change in the position of the emission band and hence confirms the existence of a particular energy band. The assynthesized g-C_3N_4 film exhibited stable and strong photoluminescence emission centered around 450-460 nm. The photoluminescence lifetime analysis as detected from the time decay spectra suggest this free-standing g-C3N4 film as a prospective candidate for bioimaging and display applications.

Acknowledgement :

I would like to thank Prof. Shyamal Kumar Saha Sir who gave me this opportunity to work on this project. I got to learn a lot from this project about Nanomaterials. I would also like to thank our teacher Tapas Kumar Mondal Sir. At last, I would like to extend my heartfelt thanks to my parents because without their help this project would not have been successful. Finally, I would like to thank my dear friends who have helped me a lot all the time.

References

[1] Y. Wang, X. Wang and M. Antonietti, Angew. Chem., Int. Ed., 2012, 51, 68

[2] J. Lu, J.-x. Yang, J. Wang, A. Lim, S. Wang and K. P. Loh, ACS Nano, 2009, 3, 2367.

[3] V. N. Khabashesku, J. L. Zimmerman and J. L. Margrave, Chem. Mater., 2000, 12, 3264

[4] X. Li, G. Hartley, A. J. Ward, P. A. Young, A. F. Masters and T. Maschmeyer, The Journal of Physical Chemistry C, 2015, 119, 14938-14946.

[5] M. Deifallah, P. F. McMillan and F. Corà, The Journal of Physical Chemistry C, 2008, 112, 5447- 5453.

[6] F. Dong, L. Wu, Y. Sun, M. Fu, Z. Wu and S. C. Lee, Journal of Materials Chemistry, 2011, 21, 15171-15174.